Theory of the non-steady-state photoelectromotive force for a two-level model of a photoconductor

M. A. Bryushinin
Institute of Problems of Mechanical Engineering, Russian Academy of Sciences, 199178, St. Petersburg, Russia

I. A. Sokolov*
A. F. Ioffe Physical Technical Institute, Russian Academy of Sciences, 194021, St. Petersburg, Russia
and Institute of Problems of Mechanical Engineering, Russian Academy of Sciences, 199178, St. Petersburg, Russia
(Received 6 March 2000)

The excitation of the non-steady-state photoelectromotive force is considered for the model of semiconductor with two impurity levels from which photocarriers are generated. The general expressions for complex amplitudes of photocurrent and electric field are obtained. We analyze the dependencies of photoelectromotive force signal amplitude on temporal and spatial frequencies for the sillenite-type crystals and present a possible way for determination of real photoelectric parameters (the lifetime of carriers, their mobility, and average diffusion length).

I. INTRODUCTION

Photorefractive sillenites $Bi_{12}Si(Ge,Ti)O_{20}$ are promising materials for optical signal processing due to their high sensitivity.[1] Large electrooptic coefficient allows an easy observation of the internal electric field. Shallow traps play significant role in the process of hologram formation. Recording and erasing processes have several time constants.[2,3] Many attempts have been started in order to determine the charge-carrier mobility, which is among the most important parameters of the light-induced charge transport. For photorefractive sillenites electron mobility values measured by various techniques from 5.2×10^{-9} to 3.4×10^{-4} $m^2\,V^{-1}\,s^{-1}$ have been reported.[4–8] This scattering of the data is usually attributed to the influence of shallow traps which reduce the average velocity of excited carriers.

The effect of non-steady-state photoelectromotive force (photo-EMF) is the holographic related phenomenon and the influence of shallow traps on the photocurrent generation in photorefractive sillenites grown in an oxygen-free atmosphere has already been revealed.[9] The non-steady-state photo-EMF is observed as an alternating electrical current flowing through the short-circuited photoconductive sample illuminated by an oscillating light pattern.[10] This photocurrent is resulted from periodic modulation of the spatial shift between the sinusoidal distribution of photoconductivity, which follows movements of the recording interference pattern, and that of the stationary space-charge electric field. The dependencies of the photocurrent on spatial and temporal frequencies allow the determination of important photoelectric parameters such as the sign of carriers, their average diffusion length, and lifetime, the Debye screening length and the photoconductivity of the crystal.[10,11]

In this paper we analyze the effect of non-steady-state photo-EMF for the model of photoconductor with a shallow level and consider application of this method for determination of material parameters. In Sec. II, we present the general expressions for the electric field and non-steady-state photocurrent amplitudes obtained for the small contrast m of the interference pattern ($m\ll1$) and small amplitude of phase modulation ($\Delta\ll1$). In Sec. III, we apply the solution for low illumination intensities when the shallow level is filled slightly, and in Sec. IV we consider the situation of strong filling of shallow level.

II. ELECTRIC FIELD AND PHOTOCURRENT AMPLITUDES

This section presents calculations of the non-steady-state photo-EMF amplitude for the simplest two-level model of semiconductor with electron photoconductivity. Photocarriers are excited from the deep donor levels (with the total density N_D) and from the shallow levels (with the total density M_T) [Fig. 1(a)]. The deep donors are ionized by light radiation only, for the shallow traps both the light and thermal mechanisms of activation are possible. The shallow level is assumed to be empty in the dark and the deep donor level is partially filled (with the density of vacant states N_A). The balance equations for this model can be written as follows:[12]

$$\frac{\partial N}{\partial t}=S_D I(N_D-N_A-N)-\gamma_D n(N_A+N), \tag{1}$$

$$\frac{\partial M}{\partial t}=-(\beta+S_T I)M+\gamma_T n(M_T-M). \tag{2}$$

Here N is the density of deep centers emptied by light ($N_D^+=N_A+N$ is the total concentration of ionized donors), M is the density of shallow centers filled with electrons, n is the density of free electrons, S_D and S_T are the light excitation

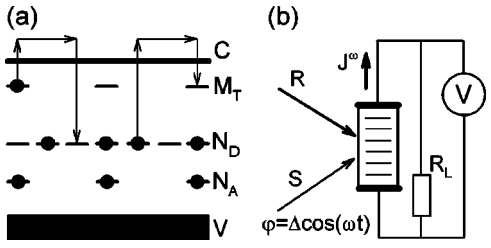

FIG. 1. The model of a photoconductor with shallow level (a) and the conventional scheme of holographic photocurrent measurements (b).

 ©2000 The American Physical Society

cross sections for deep and shallow levels, β is the thermal excitation rate from shallow level, γ_D and γ_T are the recombination constants for deep and shallow traps, respectively, I is the light intensity.

For calculation of photocurrent amplitude kinetic Eqs. (1), and (2) should be added by the continuity and Poisson's equations and by the expression for the current density:

$$\frac{\partial}{\partial t}(N-M-n)+\frac{1}{e}\mathrm{div}\ \mathbf{j}=0, \tag{3}$$

$$\mathrm{div}\,\mathbf{E}=\frac{e}{\epsilon\epsilon_0}(N-M-n), \tag{4}$$

$$\mathbf{j}=e\mu n\mathbf{E}+eD\,\mathrm{grad}\,n. \tag{5}$$

Here $\mathbf{j}$ is the current density, $\mathbf{E}$ is the electric field, μ is the electron mobility, $D=(k_BT/e)\mu$ is the diffusion coefficient, ϵ is the dielectric constant of the medium, ϵ_0 is the permittivity of free space, e is the electron charge.

Let us consider the excitation of the non-steady-state photo-EMF with an oscillating interference pattern formed by two coherent plane waves one of which is phase modulated with frequency ω and amplitude Δ [Fig. 1(b)]:

$$I(x,t)=I_0\{1+m\cos[Kx+\Delta\cos(\omega t)]\}. \tag{6}$$

Here I_0 is the average light intensity, m is the contrast, and K is the spatial frequency of the interference pattern.[10] For small contrast of the interference pattern m and small amplitude of phase modulation Δ ($m\ll 1,\Delta\ll 1$) the intensity distribution (6) can be written as[13]

$$\begin{aligned}I(x,t)=I_0+I^{+0}\exp(iKx)+I^{-0}\exp(-iKx)+I^{++}\\ \times\exp[i(Kx+\omega t)]+I^{+-}\exp[i(Kx-\omega t)]+I^{-+}\\ \times\exp[i(-Kx+\omega t)]+I^{--}\exp[i(-Kx-\omega t)],\end{aligned} \tag{7}$$

where

$$I^{+0}=I^{-0}=\frac{m}{2}I_0,$$

$$I^{++}=I^{+-}=-I^{-+}=-I^{--}=\frac{im\Delta}{4}I_0. \tag{8}$$

We shall look for the solution of Eqs. (1)–(5) in the form of identical decompositions for $N(x,t)$, $M(x,t)$, $n(x,t)$, $E(x,t)$ as it was done for the intensity distribution. All the necessary complex amplitudes for N, M, n, and E have been found and the most important of them can be written as follows:

$$n^{\pm 0}=\frac{m}{2}\,\frac{S_DI_0(N_D-N_A-N_0)T_D+S_TI_0M_0T_T}{1+T_D/\tau_D+T_T/\tau_T+\tau_MDK^2}, \tag{9}$$

$$n^{\pm +}=\frac{\pm im\Delta}{4}\,\frac{S_DI_0(N_D-N_A-N_0)T_D/(1+i\omega T_D)+S_TI_0M_0T_T/(1+i\omega T_T)}{1+T_D/[\tau_D(1+i\omega T_D)]+T_T/[\tau_T(1+i\omega T_T)]+\tau_MDK^2/(1+i\omega\tau_M)}, \tag{10}$$

$$E^{\pm 0}=\frac{\mp imE_d}{2n_0}\,\frac{S_DI_0(N_D-N_A-N_0)T_D+S_TI_0M_0T_T}{1+T_D/\tau_D+T_T/\tau_T+\tau_MDK^2}, \tag{11}$$

$$E^{\pm +}=\frac{m\Delta E_d}{4n_0}\,\frac{S_DI_0(N_D-N_A-N_0)T_D/(1+i\omega T_D)+S_TI_0M_0T_T/(1+i\omega T_T)}{\{1+T_D/[\tau_D(1+i\omega T_D)]+T_T/[\tau_T(1+i\omega T_T)]\}(1+i\omega\tau_M)+\tau_MDK^2}. \tag{12}$$

Here N_0, M_0, n_0 are the stationary and spatial uniform concentrations, $E_d=(k_BT/e)K$ is the diffusion field, $\tau_M=\epsilon\epsilon_0/\sigma_0$ is the Maxwell relaxation time, $\sigma_0=e\mu n_0$ is the average photoconductivity,

$$T_D=(S_DI_0+\gamma_Dn_0)^{-1},$$

$$T_T=(\beta+S_TI_0+\gamma_Tn_0)^{-1} \tag{13}$$

are the inverse values of the sum of the generation and ion recombination rates for deep and shallow levels,[14]

$$\tau_D=[\gamma_D(N_A+N_0)]^{-1},$$

$$\tau_T=[\gamma_T(M_T-M_0)]^{-1} \tag{14}$$

are the recombination times of the electrons to the deep and shallow traps. Note that the obtained relation for the electric field (12) can also be useful for the analysis of two-wave mixing in photorefractive materials.[1]

The total photocurrent through the short-circuited sample (for cyclic boundary conditions) is defined by the drift component of current density averaged over the interelectrode spacing L:[10]

$$j(t)=\frac{1}{L}\int_0^L e\mu n(x,t)E(x,t)dx. \tag{15}$$

As follows from Eq. (15) the contribution to the first harmonic (with frequency ω) of the non-steady-state photocurrent density amplitude is produced only by the following combination of coefficients:

$$j^{\omega}=2e\mu(n^{++}E^{-0}+n^{-+}E^{+0}+n^{+0}E^{-+}+n^{-0}E^{++}). \tag{16}$$

Finally, for the complex amplitude of the current density we obtain the following expression:

$$j^{\omega}=-\frac{m^2\Delta\sigma_0 E_d i\omega\tau_M}{2n_0^2}\frac{S_D I_0(N_D-N_A-N_0)T_D+S_T I_0 M_0 T_T}{1+T_D/\tau_D+T_T/\tau_T+\tau_M D K^2}$$
$$\times\frac{S_D I_0(N_D-N_A-N_0)T_D/(1+i\omega T_D)+S_T I_0 M_0 T_T/(1+i\omega T_T)}{\{1+T_D/[\tau_D(1+i\omega T_D)]+T_T/[\tau_T(1+i\omega T_T)]\}(1+i\omega\tau_M)+\tau_M D K^2}. \tag{17}$$

It is important to point out that all expressions for the electric field and photocurrent amplitude were obtained with the only approximation of small contrast m and amplitude of phase modulation Δ (no assumptions were made about the occupancy of the deep and shallow levels and the prevalence of any activation mechanism for the shallow level).

III. LOW INTENSITY APPROXIMATION

A. Stationary photoconductivity of the crystal

The expression for the complex amplitude of the photo-EMF [Eq. (17)] contains stationary and spatially uniform concentrations N_0, M_0, and n_0 that appear in the sample under uniform illumination with the average intensity I_0. The values N_0, M_0, and n_0 are calculated from Eqs. (1) and (2) and the neutrality condition:

$$N_0=M_0+n_0. \tag{18}$$

In this section we consider the situation of low illumination levels, i.e., slight filling of the shallow level:

$$M_0\ll M_T. \tag{19}$$

The strong filling of the shallow level makes the effective mobility and lifetime tend to their real values,[15] this situation is considered separately in Sec. IV.

The simplest solution of Eqs. (1), (2), and (18) can be obtained in the case of linear generation from the deep level

$$N_0\ll N_D-N_A \tag{20}$$

and predominance of the thermal activation of shallow traps under light excitation

$$S_T I_0\ll\beta. \tag{21}$$

The assumption (20) means that we neglect light-induced changes in absorption.[12] If conditions (19)–(21) are satisfied the concentrations N_0, n_0 equal

$$N_0=\sqrt{\frac{N_A^2}{4}+\frac{S_D I_0(N_D-N_A)}{\gamma_D}\left(1+\frac{M_T}{N_{CM}}\right)}-\frac{N_A}{2}, \tag{22}$$

$$n_0=\frac{N_0}{(1+M_T/N_{CM})}, \tag{23}$$

where

$$N_{CM}=\beta/\gamma_T=N_C\exp[-E_T/(k_B T)] \tag{24}$$

is the effective density of states in the conduction band calculated with respect to the energy position of shallow traps,[15] N_C is the effective density of states in the conduction band, E_T is the energy depth of the shallow level, k_B is the Boltzmann constant, T is the absolute temperature.

The concepts of real and effective photoelectric parameters were considered elsewhere.[2,15] For the considered model, the relation between effective and real parameters is the following:

$$\mu/\mu'=\gamma_D/\gamma_D'=(1+M_T/N_{CM}). \tag{25}$$

This expression denotes that all the values containing N_0 (e.g., Debye screening length L_S), μn_0 product (e.g., average photoconductivity σ_0) and $\mu\gamma_D^{-1}$ product (e.g., diffusion length L_D) can be written using either real or effective parameters.

There are two significant types of intensity dependencies of n_0 and N_D^+ (and as a consequence, photoconductivity, and effective lifetime of carriers). If the intensity of the incident radiation is small enough, so that $N_0\ll N_A$, the effective lifetime $\tau'=(\gamma_D' N_D^+)^{-1}$ is independent on light intensity and photoconductivity is the linear function of light intensity ($\sigma_0\propto I_0$). For the opposite situation, i.e., for $N_0\gg N_A$ (the case of quadratic recombination), the quantities σ_0 and τ' depend on the intensity as: $\sigma_0, 1/\tau'\propto I_0^{0.5}$.

B. Frequency transfer function of the photo-EMF

As seen the general expression (17) is rather complicated for further analysis, so we shall consider the frequency transfer function of the photo-EMF under certain simplifying assumptions. Three of them, i.e., Eqs. (19)–(21), were made when we calculated the spatially uniform concentrations. The fourth condition can be written as follows:

$$S_T M_0\ll S_D(N_D-N_A). \tag{26}$$

This is the case when the light excitation of free carriers from the deep level is more effective than the light excitation from the shallow one. Another condition can be written as

$$\beta T_D\gg 1. \tag{27}$$

This condition states that the number of free carriers excited from the shallow level during characteristic time T_D is larger than the number of carriers captured at this level [for $N_D\gg N_A+N_0$ the value T_D is nearly equal to the lifetime of

ionized deep level, i.e., $T_D \approx (\gamma_D n_0)^{-1}$]. Under these simplifying assumptions the expression for the photocurrent amplitude is the following:

$$j^{\omega} = \frac{-0.5m^2\Delta\sigma_0 E_d(1+\Theta+K^2L_S^2)^{-1} i\omega\tau_M}{1+\Theta+K^2L_S^2-\omega^2\tau_M\tau'+i\omega[\tau'+\tau_M(1+\Theta+K^2L_D^2)]}. \tag{28}$$

Here

$$L_D = \sqrt{\mu\tau_D k_B T/e} \tag{29}$$

is the average diffusion length of photocarriers (corresponding to deep traps),

$$\tau' = \tau'(\omega) = \tau_D\left(1+\frac{M_T/N_{CM}}{1+i\omega\beta^{-1}}\right) \tag{30}$$

is complex and frequency-dependent effective electron lifetime,

$$L_S = \sqrt{\frac{\epsilon\epsilon_0 k_B T}{e^2(N_A+N_0)(1-N_A/N_D)}} \tag{31}$$

is the Debye screening length,[12,13]

$$\Theta = [(1+N_A/N_0)(1-N_A/N_D)]^{-1} \tag{32}$$

is the dimensionless parameter ($0<\Theta<1$). This parameter characterizes the type of captures to the deep level: $\Theta \ll 1$ for linear recombination ($N_0 \ll N_A, \sigma_0 \propto I_0$) and Θ tends to 1 for quadratic recombination ($N_0 \gg N_A, \sigma_0 \propto I_0^{0.5}$).

For the numerical calculations of the photo-EMF we use the following parameters:[1,2,8,16]

$$N_D = 1\times10^{25}\ \mathrm{m}^{-3}, \quad N_A = 0.95\times10^{22}\ \mathrm{m}^{-3},$$

$$M_T = 10^{20}-10^{21}\ \mathrm{m}^{-3}, \quad \mu = 3.4\times10^{-4}\ \mathrm{m}^2\,\mathrm{V}^{-1}\,\mathrm{s}^{-1},$$

$$S_D = 1.06\times10^{-5}\ \mathrm{m}^2\,\mathrm{J}^{-1}, \quad \beta^{-1} = 2\times10^{-7}\ \mathrm{s},$$

$$\gamma_D' = 1.65\times10^{-17}\ \mathrm{m}^3\,\mathrm{s}^{-1}, \quad \tau_T = 4\times10^{-9}\ \mathrm{s}. \tag{33}$$

Conditions (19)–(21), (26), and (27) are satisfied for moderate light intensities $I_0 = 0-3\times10^4\ \mathrm{W/m}^2$. It is useful to write the values contained in Eq. (28) and calculated for $I_0 = 10^4\ \mathrm{W/m}^2$:

$$\tau_D = 1.3\times10^{-7}\ \mathrm{s}, \quad \tau'(0) = 6.4\times10^{-6}\ \mathrm{s},$$

$$\tau_M = 6.9\times10^{-5}\ \mathrm{s}, \quad T_D = 9.0\times10^{-3}\ \mathrm{s},$$

$$T_T = 2.0\times10^{-7}\ \mathrm{s}, \quad L_D = 1.0\times10^{-6}\ \mathrm{m},$$

$$L_S = 9.1\times10^{-8}\ \mathrm{m}, \quad \Theta = 7.1\times10^{-4}. \tag{34}$$

Note that $T_T = \beta^{-1}$ if assumptions (19) and (21) take place. As seen conditions $\tau_T \ll \beta^{-1} \sim \tau_D \ll \tau'(0) \ll \tau_M \ll T_D$, $L_S \ll L_D$, $\Theta \ll 1$ are satisfied.

The frequency dependencies of the photocurrent amplitude and its phase are shown in Figs. 2 and 3. The curve $|j^{\omega}(\omega)|$ has one growing, two frequency independent, and two decreasing regions.

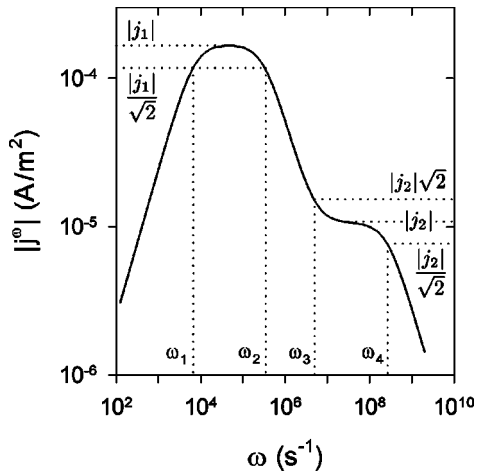

FIG. 2. The theoretical dependence of the photocurrent amplitude j^{ω} versus frequency of phase modulation ω ($I_0 = 10^4\ \mathrm{W/m}^2$, $K = 10^6\ \mathrm{m}^{-1}$, $m = 0.2$, $\Delta = 0.1$).

The linear growth at low frequencies following by the frequency independent region has the standard explanation.[10,13] For low oscillation frequencies ω both the photoconductivity and electric-field gratings follow the movements of the interference pattern. This results in a small value of periodical spatial shifts between these distributions, and as a consequence, in a small amplitude of the output electrical signal.

In order to clarify this situation let us consider the frequency dependencies of complex amplitudes n^{-0}, n^{++}, E^{-0}, E^{++} (Fig. 4) and estimate their relative contribution to the total current (16). As seen from Figs. 4(a) and (b) for $\omega \ll \omega_1$ the following relation between corresponding complex amplitudes n^{-0}, n^{++}, E^{-0}, E^{++} is valid: $|n^{++}E^{-0}| \approx |n^{-0}E^{++}|$ (or $|n^{-0}/n^{++}| \approx |E^{-0}/E^{++}|$). However, the phases of products $n^{++}E^{-0}$ and $n^{-0}E^{++}$ are opposite [Fig. 4(c)] and these components compensate each other resulting in a small photocurrent amplitude. If the frequency of phase modulation is increased the oscillation amplitudes n^{++} and E^{++} become smaller with the faster decrease of the latter component [Figs. 4(a) and (b)]. Besides an additional phase shift appears between them [Fig. 4(c)]. Finally we have $n^{++}E^{-0} + n^{-0}E^{++} \propto -i\omega\tau_M$ for $\omega < \omega_1$. The first cutoff frequency ω_1 is defined as

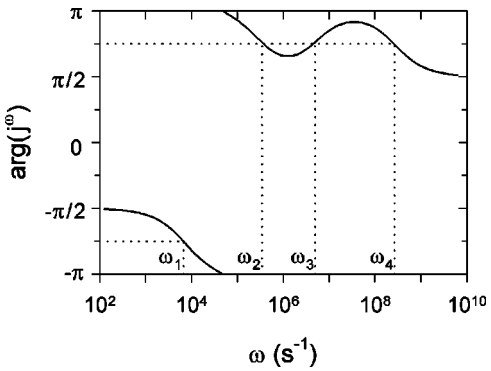

FIG. 3. The frequency dependence of the photocurrent phase ($I_0 = 10^4\ \mathrm{W/m}^2$, $K = 10^6\ \mathrm{m}^{-1}$, $m = 0.2$, $\Delta = 0.1$).

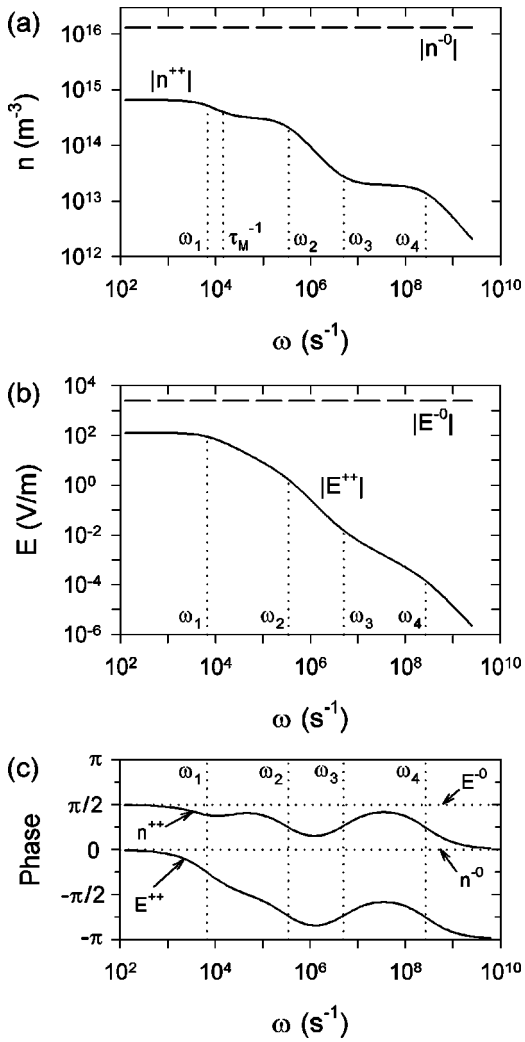

FIG. 4. Amplitudes of electron concentration (a), electric field (b), and their phases (c) versus frequency of phase modulation ω ($I_0=10^4$ W/m^2, $K=10^6$ m^{-1}, $m=0.2$, $\Delta=0.1$).

$$\omega_1 \approx \frac{1+\Theta+K^2L_S^2}{\tau'(0)+\tau_M(1+\Theta+K^2L_D^2)}. \tag{35}$$

For the ''relaxation type'' photoconductor [$\tau'(0)\ll\tau_M$] and for oscillation frequencies $\omega>\tau_M^{-1}$ the electric-field grating can be considered as ''frozen in'' (i.e., $|n^{++}E^{-0}|>|n^{-0}E^{++}|$), the amplitude of the photocurrent reaches its maximum $|j^{\omega}|\propto|n^{++}E^{-0}|$ and becomes frequency independent up to the second characteristic frequency ω_2 [Figs. 2 and 4(a)]:

$$\omega_2 \approx \frac{1}{\tau_M}+\frac{1+\Theta+K^2L_D^2}{\tau'(0)}+\frac{1+\Theta+K^2L_S^2}{\tau'(0)+\tau_M(1+\Theta+K^2L_D^2)}. \tag{36}$$

In the ''lifetime'' regime [$\tau'(0)\gg\tau_M$] relation $|n^{++}E^{-0}|\approx|n^{-0}E^{++}|$ maintain for $\omega<\omega_2\approx\tau_M^{-1}$ and dependence $n^{++}E^{-0}+n^{-0}E^{++}\propto -i\omega\tau_M$ is expected but both complex amplitudes n^{++} and E^{++} decrease as $1/\omega$ for $\omega>\omega_1\approx\tau'(0)^{-1}$ giving a plateau between ω_1 and ω_2.

The photocurrent amplitude for the first plateau for both ''relaxation'' and ''lifetime'' regimes can be written as follows:

$$j_1 \approx \frac{-0.5m^2\Delta\sigma_0E_d(1+\Theta+K^2L_S^2)^{-1}}{1+\Theta+\tau'(0)/\tau_M+K^2L_D^2}. \tag{37}$$

The photo-EMF signal peaks at modulation frequency equal to

$$\omega_{m1} \approx \sqrt{\frac{1+\Theta+K^2L_S^2}{\tau_M\tau'(0)}}. \tag{38}$$

For high excitation frequencies $\omega>\omega_2$ the photocurrent amplitude falls down because of corresponding decrease of the photoconductivity grating amplitude n^{++} [Fig. 4(a)]. There are two regions on the frequency dependence of photocurrent where the signal amplitude decreases inversely proportional to the frequency of phase modulation ($\propto 1/\omega$). This behavior is associated with the frequency dependence of the effective electron lifetime τ'. As seen from Eq. (30) there are two frequency regions where the effective lifetime τ' is real and frequency independent:

$$\tau' \approx \tau'(0)=\tau_D(1+M_T/N_{CM}) \tag{39}$$

for excitation frequencies much smaller than the thermal excitation rate from the shallow level ($\omega\ll\beta$) and

$$\tau' \approx \tau_D \tag{40}$$

for high excitation frequencies $\omega\gg\tau_T^{-1}$. The parameter $\tau'(0)$ was introduced earlier in Ref. 15 as a time constant describing the process of photoconductivity relaxation in semiconductor with shallow traps. When the crystal is illuminated with square modulated light the photocurrent pulse response has two characteristic regions: fast and slow.[15] The fast part starts immediately after illumination is switched on and associated with the process of establishment of thermal equilibrium between the shallow level and conduction band. The second (slow) region is observed under quasi steady-state condition and has characteristic time $\tau'(0)$.

The frequency dependence of the photo-EMF signal for $\omega>\beta$, as seen from Fig. 2, has another frequency independent region lying between two characteristic frequencies. The first one is equal to

$$\omega_3 \approx \beta \tag{41}$$

and the second one (for $\beta\gg\tau_M^{-1}$) can be written as

$$\omega_4 \approx \frac{1+\Theta+K^2L_D^2}{\tau_D}+\frac{1}{\tau_T}. \tag{42}$$

One can see that the expressions for ω_2 and ω_4 have similar forms for the case of ''relaxation-type'' photoconductor [$\tau'(0)\ll\tau_M$], linear photoconductivity ($\Theta\ll1$), and low spatial frequencies ($KL_D<1$). The second cutoff frequency ω_2 equals the inverse relaxation time of photoconductivity, i.e., $\omega_2\approx\tau'(0)^{-1}$, whereas the fourth one ω_4 equals the inverse actual lifetime of electrons in the conduction band, i.e., $\omega_4\approx\tau_D^{-1}+\tau_T^{-1}$.

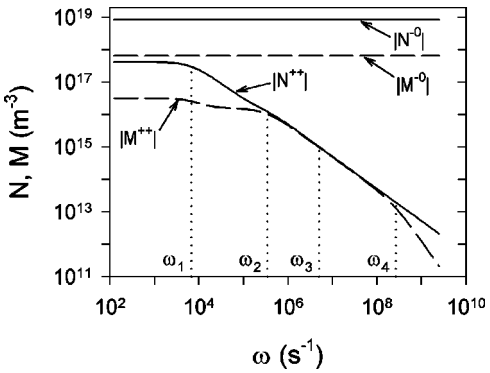

FIG. 5. Amplitudes of densities N and M versus frequency of phase modulation ω ($I_0=10^4$ W/m^2, $K=10^6$ m^{-1}, $m=0.2$, $\Delta=0.1$).

The photocurrent amplitude in the frequency range $\omega_3<\omega<\omega_4$ can be written as

$$j_2\approx\frac{-0.5m^2\Delta\sigma_0E_d(1+\Theta+K^2L_S^2)^{-1}}{1+\Theta+\tau_D/\tau_M+\tau_D/\tau_T+K^2L_D^2}. \tag{43}$$

The existence of such a plateau on the frequency transfer functions of the photo-EMF (Fig. 2) and photoconductivity [Fig. 4(a)] can be explained as follows: the analysis of the effect shows that photocurrent signal is proportional to $(\omega\tau')^{-1}$ for modulation frequencies $\omega>\omega_2$. In the frequency range $\beta<\omega<\tau_T^{-1}$ the value $|\tau'|$ depends on frequency as ω^{-1} [see Eq. (30)] so the photocurrent and photoconductivity amplitudes remain approximately constant here.

The frequency dependencies of complex amplitudes N and M are shown in Fig. 5. As seen dependencies $|M^{++}(\omega)|$ and $|n^{++}(\omega)|$ are similar in the frequency range $\omega<\omega_3$ (in fact, $M^{++}\approx n^{++}T_T/\tau_T$). It means that space charge waves $en^{++}\exp(iKx+i\omega t)$ and $eM^{++}\exp(iKx+i\omega t)$ are summed for these frequencies and this sum can be considered as an effective wave of space charge traveling in the conduction band of the crystal characterized with the effective parameters μ', γ_D'. For frequencies $\omega>\omega_4$ we have $n^{++}\approx N^{++}$.

For the frequency range $\omega\ll\beta$ we can use the results obtained before, since expression (28) with $\tau'=\tau'(0)$ has the form similar to Eq. (19) in Ref. 13. There are still, however, minor differences associated with definition of L_S and Θ. The photo-EMF signal in this frequency range can be characterized by maximum amplitude j_1 and corresponding cutoff frequencies ω_1, ω_2.[13] At these frequencies the photocurrent amplitude decreases by a factor of $1/\sqrt{2}$ (Fig. 2) and its phase equals to $-3\pi/4$ and $3\pi/4$ (Fig. 3).

The maximum amplitude j_1 and the cutoff frequencies ω_1, ω_2 are the values of interest since having been measured they allow to estimate the Maxwell relaxation time τ_M, effective lifetime $\tau'(0)$, diffusion length L_D, parameter Θ and the effective mobility $\mu'=eL_D^2/[k_BT\tau'(0)]$. Parameters τ_M, $\tau'(0)$, L_D can be obtained from the spatial frequency dependencies of characteristic frequencies $\omega_1(K)$ and $\omega_2(K)$. For the case of ''relaxation-type'' photoconductor $[\tau'(0)\ll\tau_M]$, linear photoconductivity ($\Theta\ll1$) and low spatial frequencies ($KL_D, KL_S<1$) we have $\omega_1\approx\tau_M^{-1}$, $\omega_2\approx\tau'(0)^{-1}$, and at spatial frequency $K=L_D^{-1}$ these cutoff frequencies change by a factor of 2: $\omega_1(K=L_D^{-1})=0.5\omega_1(K\approx0)$, $\omega_2(K=L_D^{-1})=2\omega_2(K\approx0)$. The value of diffusion length L_D can be also directly estimated from the dependence $j_1(K)$ (this topic is considered in Sec. III C). As it follows from Eqs. (13), (14), (23), (32), and (39) the value Θ can be expressed as the following ratio: $\Theta=\tau'(0)/T_D$. So, if the photoconductivity σ_0 depends on light intensity as $\sigma_0(I_0)\propto I_0^x$ (in the finite region near I_0) then $\Theta(I_0)=1/x-1$. This means that $\Theta(I_0)$ can be estimated from the intensity dependence $\omega_1(I_0)$ measured for low spatial frequency ($KL_D, KL_S<1$) in the crystal with $\tau'(0)\ll\tau_M$. Intensity dependence $\omega_2(I_0)$ can provide information about Θ as well. Finally, for crystal with $\tau'(0)\ll\tau_M$ and low spatial frequency ($KL_D<1$) the value Θ can be estimated as follows: $\Theta(I_0)=[\omega_2(I_0)-\omega_2(0)]/[\omega_2(I_0)+\omega_2(0)]$.

As seen from Figs. 2, 3, and Eq. (41) there is a possibility for the experimental measurement of the thermal excitation rate from the shallow level β: at frequency $\omega=\beta$ the photocurrent equals $|j^\omega|=\sqrt{2}|j_2|$ and its phase is $3\pi/4$. Furthermore, from the measured values of corresponding cutoff frequencies ω_3, ω_4 and using Eqs. (24), (39), (41), and (42) one can easily estimate the value of the electron lifetime with respect to the deep donor level

$$\tau_D\approx[1+\Theta+K^2L_D^2+\omega_3\tau'(0)]/(\omega_3+\omega_4) \tag{44}$$

and the lifetime of electrons in the conduction band

$$\tau=(\tau_D^{-1}+\tau_T^{-1})^{-1}=[\omega_4-(\Theta+K^2L_D^2)/\tau_D]^{-1}. \tag{45}$$

Besides that, from the estimated values of the diffusion length L_D and lifetime τ_D, we can easily obtain the real (band) mobility of photocarriers: $\mu=eL_D^2/[k_BT\tau_D]$.

C. Spatial frequency dependence of the photo-EMF

Let us analyze Eq. (28) for ''relaxation-type'' photoconductor $[\tau'(0)\ll\tau_M]$, for the case of linear recombination ($\Theta\ll1$) and for low-frequency range $\omega\ll\beta$. The most interesting dependencies $j^\omega(K)$ are those obtained for $\omega\ll\omega_1$ and for $\omega=\omega_{m1}$ [i.e., $j_1(K)$].

In the frequency range $\omega\ll\omega_1$ the signal amplitude can be written as

$$j^\omega(K)\propto K(1+K^2L_S^2)^{-2}. \tag{46}$$

The signal amplitude grows linearly versus spatial frequency for $KL_S<1/\sqrt{3}$ (Fig. 6, line c) which is due to increase of diffusion field amplitude E_d and decreases as $\sim K^{-3}$ for $KL_S>1/\sqrt{3}$, behavior corresponding to saturation of deep traps. The maximum on this dependence is observed for $K=(\sqrt{3}L_S)^{-1}$.

For $\omega=\omega_{m1}$ as seen from Eq. (37) we have the following expression for the signal amplitude

$$j^\omega(K)\propto K(1+K^2L_S^2)^{-1}(1+K^2L_D^2)^{-1}. \tag{47}$$

In photorefractive sillenite crystals the value of the diffusion length of electrons is usually larger than the Debye screening length, i.e., $L_D>L_S$. In this case the decrease of the signal amplitude as $\sim K^{-1}$ [see dependence $j_1(K)$ in Fig. 6, line a]

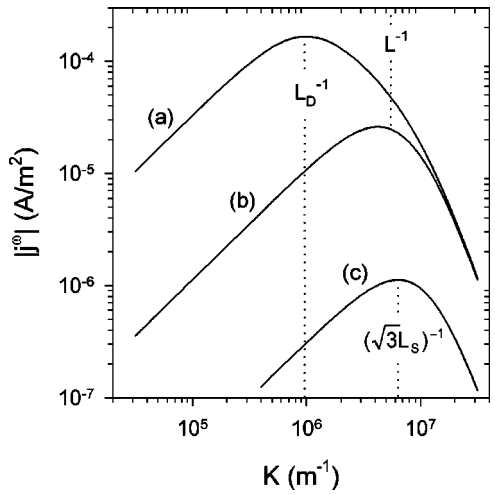

FIG. 6. The dependence of the photocurrent amplitude j^{ω} on spatial frequency K calculated for characteristic temporal frequencies: (a) $\omega_1<\omega<\omega_2$ [Eq. (37)], (b) $\omega_3<\omega<\omega_4$ [Eq. (43)], (c) $\omega \ll \omega_1$ [Eq. (28)] for $\omega/2\pi=2$ Hz; $I_0=10^4$ W/m^2, $m=0.2$, $\Delta=0.1$.

is due to smoothing of electron density distribution in the conduction band. The photocurrent amplitude peaks at spatial frequency $K\approx L_D^{-1}$.[10]

Let us analyze the spatial frequency dependence $j_2(K)$ of the photo-EMF signal for high excitation frequencies $\omega_3<\omega<\omega_4$. For $\Theta\ll 1$, $\tau_D\ll\tau'(0)\ll\tau_M$ Eq. (43) can be written in the following form:

$$j^{\omega}(K)\propto K(1+K^2L_S^2)^{-1}(1+K^2L^2)^{-1}. \tag{48}$$

Here $L=\sqrt{\mu\tau k_BT/e}$ is the actual diffusion length of electrons. If the condition $L>L_S$ is satisfied the maximum on this dependence is observed at $K\approx L^{-1}$ (Fig. 6, line b). This means that real parameters can be determined from the spatial frequency dependence of the photo-EMF signal measured in the frequency range $\omega_3<\omega<\omega_4$. Such practical estimation of real diffusion length for sillenites may be complicated because of approaching L to L_S [for the chosen material parameters (33) $L=1.8\times10^{-7}$ m and $L_S=9.1\times10^{-8}$ m].

D. Intensity dependence of the non-steady-state photo-EMF

Let us first consider the intensity dependencies of the photocurrent amplitude and corresponding cutoff frequencies for low illumination levels. The shallow level is almost empty in this case [see Eq. (19)] and all intensity dependencies of the effect are determined by behavior of the deep level. It follows from the fact that the intensity dependencies of values n_0, σ_0, τ_M, τ_D, $\tau'(0)$, L_D, L_S, Θ are expressed via the intensity dependence of the density N_0 [see Eqs. (14), (23), and (29)–(32)]. The dependence $N_0(I_0)$ (22) in its turn is almost identical to the analogous dependence for the standard model of semiconductor with one deep level.[13] The difference is described by the presence of the intensity independent factor $(1+M_T/N_{CM})$ and can be eliminated by using effective parameter γ_D' (25).

For the case of linear recombination of photocarriers ($N_0\ll N_A$) and for $\tau'(0)\ll\tau_M$ corresponding values j_1, j_2 and ω_1 [Eqs. (37), (43), and (35)] are proportional to the average light intensity I_0, other quantities, i.e., ω_2, ω_3, ω_4 [Eqs. (36), (41), and (42)], are intensity independent. It follows from the linear character of the photoconductivity $\tau_M^{-1}\propto\sigma_0\propto I_0$ and intensity independence of the other material parameters: $\tau'(0),\tau_D,\tau_T,L_D,L_S,\Theta\approx\text{const}(I_0)$.

The situation of quadratic recombination ($N_0\gg N_A$) and for $\tau'(0)\sim\tau_M$ is more complicated: all values except ω_3 are intensity dependent. This peculiarity appears due to the intensity dependencies of the material parameters: $\sigma_0,\tau_M^{-1},\tau_D^{-1},\tau'(0)^{-1},L_D^{-2},L_S^{-2}\propto I_0^{0.5}$. For low spatial frequencies ($KL_D,KL_S<1$) we have $j_1,\omega_1,\omega_2\propto I_0^{0.5}$, the character of dependencies $j_2(I_0)$, $\omega_4(I_0)$ can vary according to the relation between τ_D and τ_T. For the sillenite crystals sublinear photoconductivity dependence is observed,[17] $\tau_T\ll\tau_D$ [$\tau_T=4\times10^{-9}$ s,[1] $\tau_D\sim(3-160)\times10^{-6}$ s] and hence $j_2\propto I_0$, $\omega_4\approx\text{const}(I_0)$. The value τ_D is calculated using Eq. (39) and experimental estimations of the photoconductivity relaxation time $\tau'(0)=(0.15–8)\times10^{-3}$ s obtained for the sillenite crystals grown in an oxygen-free atmosphere.[9,17]

IV. STRONG FILLING OF SHALLOW LEVEL

A. Stationary photoconductivity of the crystal

Let us consider the signal dependence for the case of sufficient filling of the shallow level. In order to perform numerical calculations of photovoltage we have to estimate stationary and spatially uniform densities N_0, M_0, and n_0. Let us assume that the conditions of linear generation (20) and linear recombination

$$N_0\ll N_A \tag{49}$$

are satisfied for the deep level. Then the necessary concentrations are easily calculated from Eqs. (1), (2), and (18) and equal to

$$n_0=S_DI_0(N_D-N_A)/(\gamma_DN_A), \tag{50}$$

$$M_0=\frac{M_T}{1+(\beta+S_TI_0)/(\gamma_Tn_0)}, \tag{51}$$

and the quantity N_0 is defined as their sum (18). As seen from Eq. (50) the concentration of electrons in the conduction band (average photoconductivity) is proportional to the light intensity while M_0 tends to the finite value for high light intensity [compare to Eq. (15) in Ref. 12]:

$$M_{\infty}=\lim_{I_0\to\infty}M_0=\frac{M_T}{1+[S_TN_A\gamma_D]/[S_D(N_D-N_A)\gamma_T]}. \tag{52}$$

For the case

$$S_D(N_D-N_A)/S_TM_T\gg\gamma_DN_A/\gamma_TM_T \tag{53}$$

this value is close to the total density of shallow traps M_T, so the strong filling of shallow level is possible for high light intensities.

B. Effect of photo-EMF for high light intensity

In this section we analyze the effect of photo-EMF for high light intensity when the shallow level is filled substantially:

$$M_0 \approx M_T. \tag{54}$$

For arbitrary material parameters and occupancy degrees of both levels one should use the general expression [Eq. (17)] to calculate the photocurrent amplitude. Here we shall consider two interesting situations when Eq. (17) reduces to the form similar to the one-level model approximation.

Let us assume that the light excitation from the deep level strongly exceeds the light excitation from the shallow one [Eqs. (26) and (53)]. In this case the shallow level is practically totally filled with electrons. For this reason we can neglect in Eq. (17) all terms containing parameters of shallow traps and we obtain the standard expression for photocurrent amplitude:

$$j^{\omega} = \frac{-0.5m^2 \Delta \sigma_0 E_d (1+\Theta+K^2 L_S^2)^{-1} i\omega\tau_M}{1+\Theta+K^2 L_S^2 - \omega^2 \tau_M \tau_D + i\omega[\tau_D + \tau_M(1+\Theta+K^2 L_D^2)]}. \tag{55}$$

Here Θ is given by

$$\Theta = n_0/[(N_A+N_0)(1-N_A/N_D)]. \tag{56}$$

Equation (55) is identical to the photocurrent amplitude calculated for one-level model of semiconductor.[13] In this case, however, investigation of frequency transfer function $j^{\omega}(\omega)$ and dependence $j^{\omega}(K)$ can provide estimations of real (but not effective) values τ_D, L_D and μ.

We have estimated the minimal light intensity needed for sufficient filling of shallow level so that Eq. (55) is the consequence of common expression (17) in whole frequency range: $I_0 \sim 3\times 10^6$ W/m^2 (this estimation was obtained using Eqs. (18), (50), and (51) for stationary concentrations, material parameters (33) and assuming $M_T = 1\times 10^{20}$ m^{-3}, $S_T = 0$). For this intensity the shallow level is filled by 95%.

Let us consider the situation when significant light generation of electrons from the shallow level takes place:

$$S_T M_0 \sim S_D(N_D - N_A). \tag{57}$$

If $\gamma_T M_T \gg \gamma_D N_A$ the shallow level is practically filled for high light intensities [see Eq. (52)] and we can neglect the items containing τ_T in Eq. (17). The expression for the complex amplitude of photo-EMF can be written then as follows:

$$j^{\omega} = \frac{-0.5m^2 \Delta \sigma_0 E_d (1+\Theta+K^2 L_S^2)^{-1} i\omega\tau_M A(0) A(\omega)}{1+\Theta+K^2 L_S^2 - \omega^2 \tau_M \tau_D + i\omega[\tau_D + \tau_M(1+\Theta+K^2 L_D^2)]}, \tag{58}$$

where

$$A(\omega) = 1 + \frac{S_T M_0 T_T}{S_D(N_D - N_A) T_D} \frac{1+i\omega T_D}{1+i\omega T_T}. \tag{59}$$

The frequency transfer function described by Eqs. (58) and (59) is presented in Fig. 7 (curves b and c). The calculations were performed using Eqs. (18), (50), and (51) for stationary concentrations and material parameters (33). We also assumed that $M_T = 1\times 10^{20}$ m^{-3}, $S_T = 10$ m^2 J^{-1} [choosing such S_T we satisfy condition (57)]. The characteristic cutoff frequencies are given by the following expressions:

$$\omega_1 \approx \frac{1+\Theta+K^2 L_S^2}{\tau_D + \tau_M(1+\Theta+K^2 L_D^2)}, \tag{60}$$

$$\omega_2 \approx \frac{1}{T_T[1+S_T M_0/S_D(N_D-N_A)]}, \tag{61}$$

$$\omega_3 \approx \frac{1}{T_T + \tau_D/(1+\Theta+\tau_D/\tau_M+K^2 L_D^2)}, \tag{62}$$

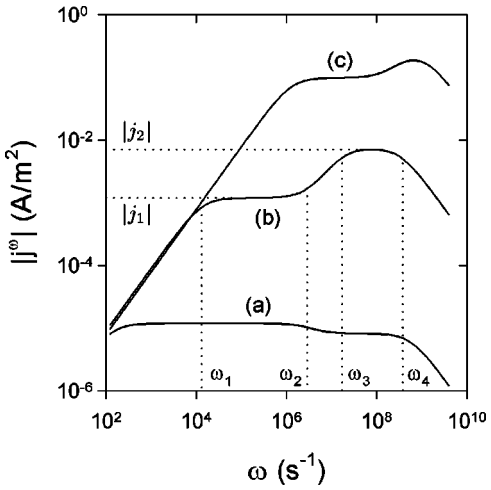

FIG. 7. The frequency transfer function of the photo-EMF for different light intensities $I_0 = 3\times 10^3$, 3×10^5, 3×10^7 W/m^2 (curves (a), (b), and (c), respectively). The calculations are performed using Eq. (17) for $K = 6.3\times 10^6$ m^{-1}, $m = 0.2$, $\Delta = 0.1$.

$$\omega_4 \approx \frac{1}{\tau_M} + \frac{1+\Theta+K^2L_D^2}{\tau_D} + \frac{1}{T_T} + \frac{1}{T_T+\tau_D/(1+\Theta+\tau_D/\tau_M+K^2L_D^2)}. \quad (63)$$

Calculating ω_2, ω_3, ω_4 we have supposed $T_T \ll \tau_D+\tau_M(1+\Theta+K^2L_D^2)$. For the considered range of light intensities $I_0=0-10^8$ W/m^2 the following relation is satisfied: $\tau_M \geqslant 30T_T$. The amplitude of the photo-EMF signal for the frequency range $\omega_3<\omega<\omega_4$ can be written as

$$j_2 \approx \frac{-0.5m^2\Delta\sigma_0 E_d A(0)[1+S_T M_0/S_D(N_D-N_A)]}{(1+\Theta+K^2L_S^2)(1+\Theta+\tau_D/\tau_M+\tau_D/T_T+K^2L_D^2)}. \quad (64)$$

For low frequencies of phase modulation ($\omega<\omega_2$) the effect of photo-EMF is described by standard expression (55) since $A(0)\approx 1$. As seen from Fig. 7 the presence of shallow traps reveals itself only for high excitation frequencies ($\omega>\omega_2$). In contrast to the low intensity approximation [$M_0 \ll M_T$, $S_T M_0 \ll S_D(N_D-N_A)$] the influence of the shallow level for the case of high light intensities [$M_0 \approx M_T$, $S_T M_0 \sim S_D(N_D-N_A)$] leads to the increase of photocurrent at high frequencies of phase modulation (compare Figs. 2 and 7).

This fact can be explained as follows: when the shallow level is filled slightly it play a role of an electron reservoir leading to the increase of the photoconductivity relaxation time and reducing the effective electron mobility. However, when this level is filled strongly the characteristic time τ_D tends to its actual value [see Eqs. (55) and (58)] and sufficient light generation from this level leads to photocurrent increase with respect to standard estimation of Eq. (55).

V. CONCLUSION

To summarize, we have analyzed the influence of shallow traps on the effect of non-steady-state photo-EMF. We have derived the general expression for amplitude of the photocurrent for apparent filling degrees of deep and shallow levels. We analyze the photocurrent behavior with respect to temporal and spatial frequencies and discuss the case of high illumination levels. The general calculations were performed for the crystal's parameters typical for photorefractive $Bi_{12}SiO_{20}$.

We believe that influence of shallow traps is not restricted to considered cases. The effect of non-steady-state photo-EMF in other photoconductive crystals (e.g., semi-insulating GaAs) with different material constants, may reveal peculiarities at other characteristic temporal and spatial frequencies.

ACKNOWLEDGMENTS

I. Sokolov thanks Alexander von Humboldt Foundation for financial support. Support by the NATO Grant No. SfP 973252 and RFBR Grant Nos. 98-03-32791 and 99-03-32768 is acknowledged.

*Present address: Institute of Physical Chemistry, University of Heidelberg, Im Neuenheimer Feld 253, D-69120 Heidelberg, Germany.

[1] M.P. Petrov, S.I. Stepanov, and A.V. Khomenko, *Photorefractive Crystals in Coherent Optical Systems*, edited by T. Tamir, Springer Series in Optical Sciences Vol. 59 (Springer-Verlag, Berlin, 1991).
[2] G. Pauliat and G. Roosen, J. Opt. Soc. Am. B **7**, 2259 (1990).
[3] F.P. Strohkendl, J. Appl. Phys. **65**, 3773 (1989).
[4] S.L. Hou, R.B. Lauer, and R.E. Aldrich, J. Appl. Phys. **44**, 2652 (1973).
[5] B.Kh. Kostyuk, A.Yu. Kudzin, and G.Kh. Sokolyanskii, Fiz. Tverd. Tela (Leningrad) **22**, 2454 (1980) [Sov. Phys. Solid State **22**, 1429 (1980)].
[6] J.P. Partanen, J.M.C. Jonathan, and R.W. Hellwarth, Appl. Phys. Lett. **57**, 2404 (1990).
[7] I.A. Sokolov and S.I. Stepanov, J. Opt. Soc. Am. B **10**, 1483 (1993).
[8] I. Biaggio, R.W. Hellwarth, and J.P. Partanen, Phys. Rev. Lett. **78**, 891 (1997).
[9] M.A. Bryushinin, A.A. Petrov, and I.A. Sokolov, Appl. Phys. Lett. **75**, 445 (1999).
[10] M.P. Petrov, I.A. Sokolov, S.I. Stepanov, and G.S. Trofimov, J. Appl. Phys. **68**, 2216 (1990).
[11] U. Haken, M. Hundhausen, and L. Ley, Phys. Rev. B **51**, 10 579 (1995).
[12] P. Tayebati and D. Mahgerefteh, J. Opt. Soc. Am. B **8**, 1053 (1991).
[13] I.A. Sokolov and S.I. Stepanov, Optik (Stuttgart) **93**, 175 (1993).
[14] G.C. Valley, IEEE J. Quantum Electron. **QE-19**, 1637 (1983).
[15] S.M. Ryvkin, *Photoelectric Effects in Semiconductors* (Consultants Bureau, New York, 1964).
[16] Ph. Refregier, L. Solymar, H. Rajbenbach, and J.P. Huignard, J. Appl. Phys. **58**, 45 (1985).
[17] E.V. Mokrushina, M.A. Bryushinin, V.V. Kulikov, A.A. Petrov, and I.A. Sokolov, J. Opt. Soc. Am. B **16**, 57 (1999).